Assembly of Large Cerium(III)-Containing Tungstotellurites(IV) Nanocluster: $[Ce_{10}Te_8W_{88}O_{298}(OH)_{12}(H_2O)_{40}]^{18-}$

Wei-Chao Chen, Chao Qin, Xin-Long Wang,* Yang-Guang Li, Hong-Ying Zang, Kui-Zhan Shao, Zhong-Min Su* and En-Bo Wang[a]

[a]*Institute of Functional Material Chemistry, Key Lab of Polyoxometalate Science of Ministry of Education, Faculty of Chemistry, Northeast Normal University, Changchun, 130024 Jilin, People's Republic of China.*

CONTENTS

Section 1 A detailed survey tellurite as heteroanions in POTs chemistry

Table S1. A detailed survey tellurite as heteroanions in POTs chemistry

Year	Polyanion Formula	Precursors	Characteristics	Ref.
1991	$[TeW_6O_{24}]^{6-}$	WO_4^{2-} TeO_2	the first examples of the Anderson-Evans type tungstotellurate	1
1998	$[(Mn^{II}(H_2O)_3)_2(Mn^{II}(H_2O)_2)_2(TeW_9O_{33})_2]^{8-}$	WO_4^{2-} TeO_2	it can be acted as homogeneous catalysts for the epoxidation of dienes	2
2001	$[(\alpha\text{-}TeW_9O_{33})_2Cu_3(H_2O)_3]^{10-}$	WO_4^{2-} Te^{4+}	dimeric, sandwich-type transition-metal-substituted POTs	3
2002	$[Fe_4(H_2O)_{10}(\beta\text{-}Te^{IV}W_9O_{33})_2]^{4-}$	WO_4^{2-} TeO_3^{2-}	iron(III)-substituted, dimeric POTs	4
2003	$[(Ni(H_2O)_3)_2(WO_2)(Ni(H_2O)_2)(TeW_9O_{33})_2]^{8-}$ $[(Zn(H_2O)_3)_2(WO_2)_{1.5}(Zn(H_2O)_2)_{0.5}(TeW_9O_{33})_2]^{8-}$ $[(Co(H_2O)_3)_2(WO_2)(Co(H_2O)_2)(TeW_9O_{33})_2]^{8-}$	WO_4^{2-} TeO_2	sandwich-type tungstotellurates	5
2003	$[(UO_2)_2(H_2O)_2(TeW_9O_{33})_2]^{12-}$	$[TeW_9O_{33}]^{8-}$	the structure of the complexes are of an unprecendented type having 'open' structures with four unsaturated oxygen atoms	6
2008	$[H_3W_{18}O_{57}(Te^{IV}O_3)]^{5-}$	$[H_3W_{18}O_{56}(Te^{VI}O_6)]^{6-}$	the pyramidal tellurite anion $Te^{IV}O_3^{2-}$ acts as a template supporting the $\{W_{18}O_{54}\}$ cage	7
2009	$[H_2Te_4W_{20}O_{80}]^{22-}$ $[NaTeW_{15}O_{54}]^{13-}$	WO_4^{2-} TeO_2	novel tungstotellurates containing two pairs of face-shared WO_6 octahedra	8
2010	$[Te_2W_{17}O_{61}]^{12-}$ $[Te_2W_{16}O_{58}(OH)_2]^{14-}$	WO_4^{2-} TeO_2	the three lacunary POMs reported herein represent	9

	$[Te_2W_{18}O_{62}(OH)_2]^{10-}$		important new well-defined precursors for functionalised POMs.	
2011	$[Pd_3(TeW_9O_{33})_2]^{10-}$ $[(WO_2)_4(Te_2W_{15}O_{54})_4]^{32-}$ $[Te_3W_{21}O_{75}]^{12-}$	WO_4^{2-} TeO_3^{2-}	molecular "layered" heteropolyoxometalate architectures	10
2011	$[W_{28}Te_8O_{112}]^{24-}$ $[W_{28}Te_9O_{115}]^{26-}$ $[W_{28}Te_{10}O_{118}]^{28-}$	WO_4^{2-} TeO_3^{2-}	a new class of macrocyclic tungstotellurite heteropolyacid cluster-squares	11
2013	$[\{(TeO_3)W_{10}O_{34}\}_8\{Ce_8(H_2O)_{20}\}(WO_2)_4(W_4O_{12})]^{48-}$	WO_4^{2-} TeO_3^{2-}	the first lanthanide-containing POTs with tellurium heteroatom	12
2014	$[Pd_6Te_{19}W_{42}O_{190}]^{40-}$	WO_4^{2-} TeO_3^{2-}	high-nuclearity palladium-rich POMs	13
2014	$[H_{10}Ag_{18}Cl(Te_3W_{38}O_{134})_2]^{29-}$ $\{[H_{13}Ag_{18}Cl(Te_3W_{38}O_{134})_2]^{26-}\}_2$ $\{[H_{15}Ag_{18}Cl(Te_3W_{38}O_{134})_2]^{24-}\}_n$ $[H_2Te_3W_{43}O_{148}]^{24-}$	WO_4^{2-} TeO_3^{2-}	time-resolved assembly of cluster-in-cluster POTs	14
2015	$[(C_4H_8Te^{IV})_3(X^{III}W_9O_{33})_2]^{12-}$ (X = As or Sb)	$C_4H_8TeI_2$	first organotellurium-containing POMs	15
2015	$[\{Mn(CO)_3\}(Mn(H_2O)_2)(Mn(H_2O)_3)(TeW_9O_{33})]_2^{6-}$	$[TeW_9O_{33}]^{8-}$	novel POM-based carbonyl manganese derivative	16
2015	$[Ce_{10}Te_8W_{88}O_{298}(H_2O)_{40}(OH)_{12}]^{18-}$	WO_4^{2-} TeO_3^{2-}	large cerium(III)-stabilized tungstotellurites(IV) nanocluster	this work

References:

[1] E. S. Ganelina (1962). *Russ. J. Inorg. Chem.*, **7**, 812; E. S. Ganelina and N. I. Nerevyatkina (1965). *Russ. J. Inorg. Chem.*, **10**, 483; R. Ripan and N. Calu (1965). *Stud. Univ. Babes-Bolyai Chem.*, **10**, 135.

[2] M. Bösing, A. Nöh, I. Loose and B. Krebs, *J. Am. Chem. Soc.*, 1998, **120**, 7252.

[3] U. Kortz, N. K. Al-Kassem, M. G. Savelieff, N. A. Al Kadi and M. Sadakane, *Inorg. Chem.*, 2001, **40**, 4742.

[4] U. Kortz, M. G. Savelieff, B. S. Bassil, B. Keita and L. Nadjo, *Inorg. Chem.,* 2002, **41**, 783–789.

[5] E. M. Limanski, D. Drewes, E. Droste, R. Böhner and B. Krebs, *J. Mol. Struc.,* 2003, **656**, 17–25.

[6] A. J. Gaunt, I. May, R. Copping, A. I. Bhatt, D. Collison,O. D. Fox, K. T. Holman and M. T. Pope, *Dalton Trans.,* 2003*,* 3009–3014.

[7] J. Yan, D.-L. Long, E. F. Wilson and L. Cronin, *Angew. Chem. Int. Ed.,* 2009, **48**, 4376–4380.

[8] A. H. Ismail, N. H. Nsouli, M. H. Dickman, J. Knez and U. Kortz, *J. Cluster Sci.,* 2009, **20,** 453–465.

[9] C. Ritchie, K. G. Alley and C. Boskovic, *Dalton Trans.*, 2010, **39**, 8872–8874.

[10] J. Gao, J. Yan, S. Beeg, D.-L. Long and L. Cronin, *Angew. Chem. Int. Ed.,* 2012, **51**, 3373–3376.

[11] J. Gao, J. Yan, S. G. Mitchell, H. N. Miras, A. G. Boulay, D.-L. Long, L. Cronin, *Chem. Sci.*, 2011, **2**, 1502–1508.

[12] W.-C. Chen, H.-L. Li, X.-L. Wang, K.-Z. Shao, Z.-M. Su and E.-B. Wang, *Chem. – Eur. J.*, 2013, **19**, 11007–11015.

[13] J. M. Cameron, J. Gao, D.-L. Long and L. Cronin, *Inorg. Chem. Front.*, 2014, **1**, 178–185.

[14] C. Zhan, J. W. Cameron, J. Gao, J. M. Purcell, D.-L. Long and L. Cronin, *Angew. Chem. Int. Ed.*, 2014, **53**, 10362–10366.

[15] B. Kandasamy, B. S. Bassil, A. Haider, J. Beckmann, B. H. Chen, N. Dalal and U. Kortz, *J. Organ. C.*, 2015, DOI: 10.1016/j.jorganchem.2015.03.004.

[16] Y. B Liu, Y. H. Zhang, P. T. Ma, Y. K. Dong, J. Y. Niu and J. P. Wang, *Inorg. Chem. Commun.*, 2015, DOI: 10.1016/j.inoche.2015.03.043.

Section 2 Synthesis, Crystal Data, and Structures of 1

2.1 Synthesis Discussion

The precise control of the one−pot reaction conditions of combining Ce^{3+} groups with the TeO_3^{2-} anion templates at proper pH was employed for the assembly of **1**. Since the TeO_3^{2-} anion templates have a lone pair of electrons and only form three bonds through oxygen atoms in trigonal configurations, they effectively give rise to "open" lacunary units instead of "closed" Keggin-type clusters, owing to the inducing effect of the lone pair of electrons. Such templates can also be viewed as "inorganic ligands" as well as linkers according to previous reports. Moreover, the electrophile Ce^{3+} groups possess highly oxophilic nature, high coordination numbers and diverse coordination geometries. Therefore, a synergistic effect between Ce^{3+} groups and the anion template effect of TeO_3^{2-} may guide the construction of unprecedented lanthanide−containing tungstotellurites(IV).

The synthetic strategy employed in the present work builds on that reported previously by some of us (see *Chem. Eur. J.* 2013, **19**, 11007; *Cryst. Growth Des.* 2014, **10**, 5099; *Chem. Asian J.* 2015, DOI:10.1002/asia.201500004). First, we chose Na_2WO_4 and Na_2TeO_3 as the W− & Te−sources. The acidification of them (W/Te molar ratio 11:1) by acetic acid was necessary and the molar ratio also plays an important role that is in accordance with the final structure: the $\{Te_8W_{88}\}$ cluster (W:Te molar ratio 11:1). Subsequently, the electrophile Ce^{3+} salts were introduced to the acid solution. Compared to the reported synthesis of tungstotellurite nanoclusters $\{Ce_8Te_8W_{88}\}$, the countercation (K^+) was not used for **1**: parallel experiment reveals that when KCl was used there were no crystals obtained but precipitation. Thus Na^+ cation was suitable for the isolated of **1**. Finally, some efficient observations during the syntheses of **1** should be mentioned: (1) The combination of Ce^{3+} groups with TeO_3^{2-} heteroanion templates seems to be a potential strategy to build novel lanthanide−containing POTs, which may be due to the inducing effect of the lone pair of electrons in TeO_3^{2-} and the diverse coordinate numbers and geometries of Ce^{3+} centers; (2) the correct choice of counteractions and the suitable molar ratio also play important roles in preparation of final architectures.

2.2 Crystal Data

Table S2. Crystal Data and Structure Refinements for **1**.

	1
Empirical formula	$H_{200}Ce_{10}Na_{18}O_{404}Te_8W_{88}$
M	25680.22
λ/Å	0.71073
T/K	296(2)
Crystal system	Triclinic
Space group	$P\bar{1}$
a/Å	20.6145(12)
b/Å	25.4599(15)
c/Å	30.7077(18)
α/°	84.6720(10)
β/°	77.4110(10)
γ/°	81.8700(10)
V/Å^3	15539.0(16)
Z	1
D_c/Mg m^{-3}	2.744
μ/mm^{-1}	17.378
$F(000)$	11138
θ Range/°	0.68–25.00
Measured reflections	90756
Independent reflections	54747
R_{int} after SQUEEZE	0.0898
obsd ($I > 2\sigma(I)$)	20284
Goodness-of-fit on F^2	0.963
$R_1(I > 2\sigma(I))$ [a]	0.0605
wR_2 (all data) [b]	0.1525

[a] $R_1 = \sum||F_o| - |F_c||/\sum|F_o|$. [b] $wR_2 = \{\sum[w(F_o^2 - F_c^2)^2]/\sum[w(F_o^2)^2]\}^{1/2}$.

Single-crystal X-ray diffraction: Single-crystal X-ray diffraction data for **1** was recorded on a Bruker Apex CCD II area-detector diffractometer with graphite-monochromated Mo$_{K\alpha}$ radiation ($\lambda = 0.71073$ Å) at 296(2) K. Absorption corrections were applied using multiscan technique and performed by using the SADABS program[1]. The structures of **1** was solved by direct methods and refined on F^2 by full-matrix leastsquares methods by using the SHELXTL package[2]. The numbers of lattice water molecules and counter cations for **1** was estimated by the results of elemental analyses, TG curves, and calculations of electron count in the voids with SQUEEZE[3].

During the refinement, all the Ce, W and Te atoms were refined anisotropically, while the rest of the cations and all of the solvent water molecules were just refined isotropically because of their unusual anisotropic thermal parameters and obvious disorder problems. H atoms on lattice water molecules cannot be found from the residual peaks and were directly included in the final molecular formula. The 'omit -3 50' command was used to omit the weak reflections above 50 degree. The highest residual peak is 3.845 eÅ^{-3} and the deepest hole is -2.613 eÅ^{-3}. About 4 solvent water molecules and 2 Na$^+$ cations were found crystallographically; based on the TGA curve, BVS calculations and elemental analyses, another 50 water molecules, 16 Na$^+$ cations and 20 H$^+$ were included into the molecular formula directly. The void is large enough and contains enough electronic density to accommodate all Na$^+$/H$_2$O that cannot be determined crystallographically.

References:

[1] Sheldrick, G. *SADABS*; ver. 2.10; University of Gottingen: Göttingen, Germany, **2003**.

[2] Sheldrick, G. M. *SHELXL-97, Program for the Refinement of Crystal Structure*; University of Gottingen: Göttingen, Germany, **1993**.

[3] Spek, A. L. *PLATON, A Multipurpose Crystallographic Tool*; Utrecht University, Utrecht, The Netherlands, **2003**.

2.3 Structures of 1

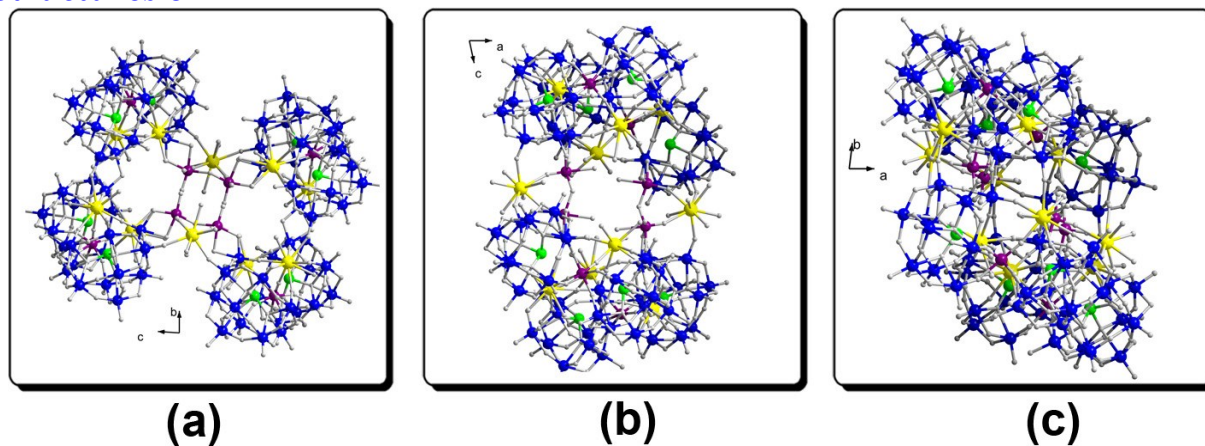

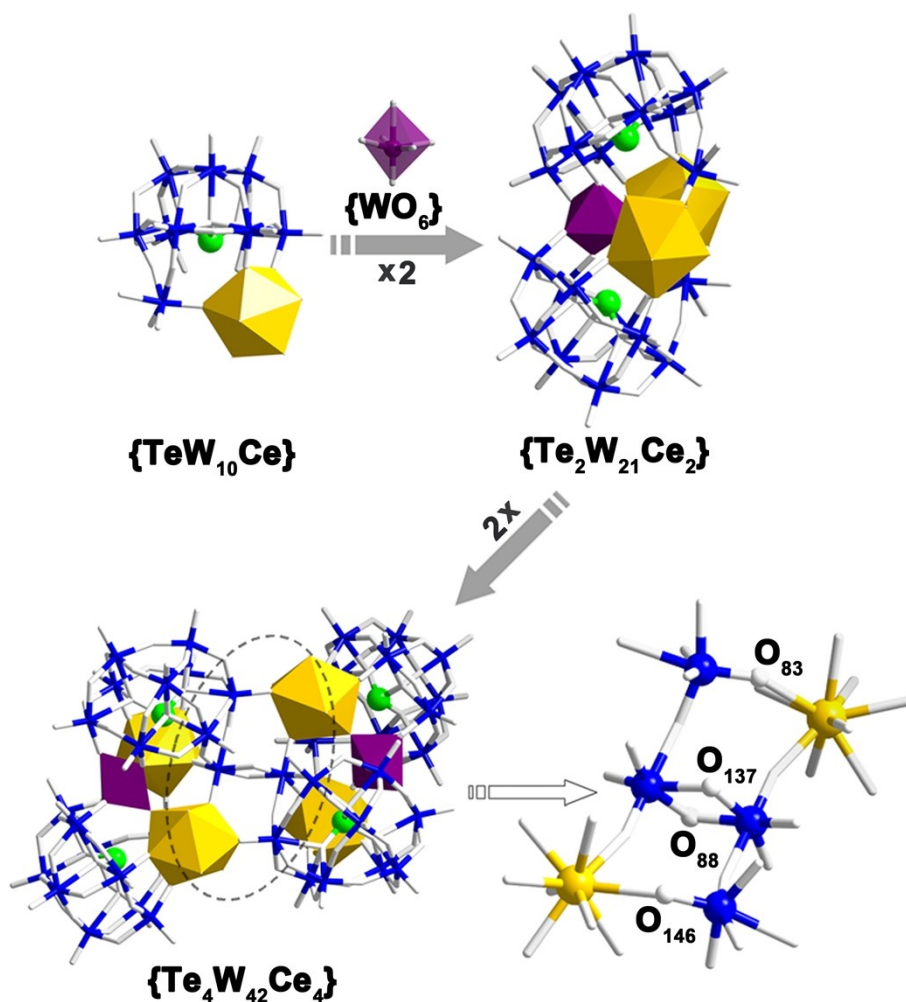**Fig. S1.** Structure of anionic cluster (**1a**) in different orientations: (a) bc-view, (b) ac-view, (c) ab-view.
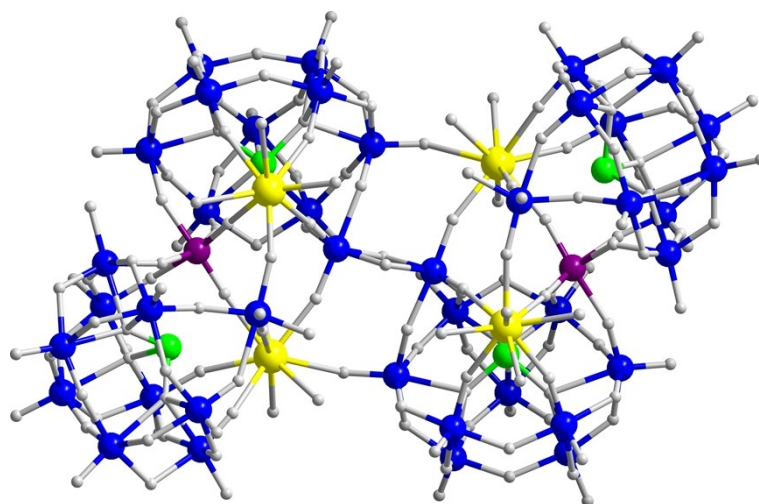

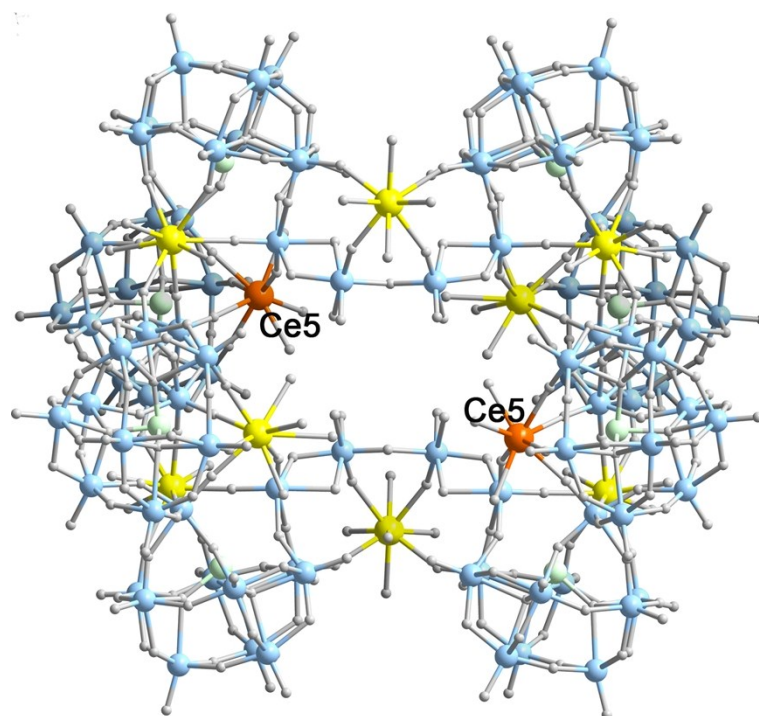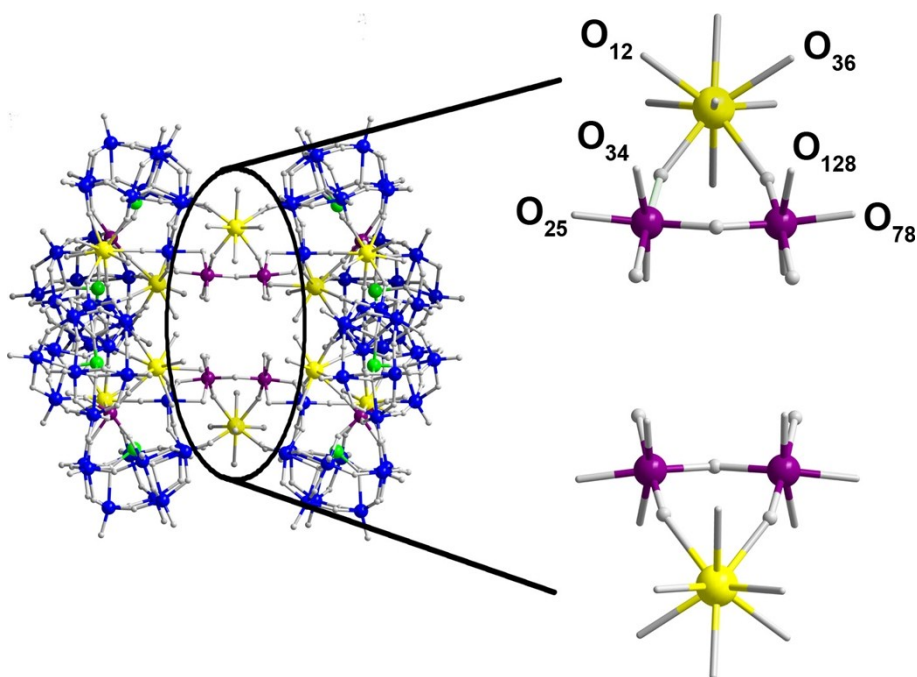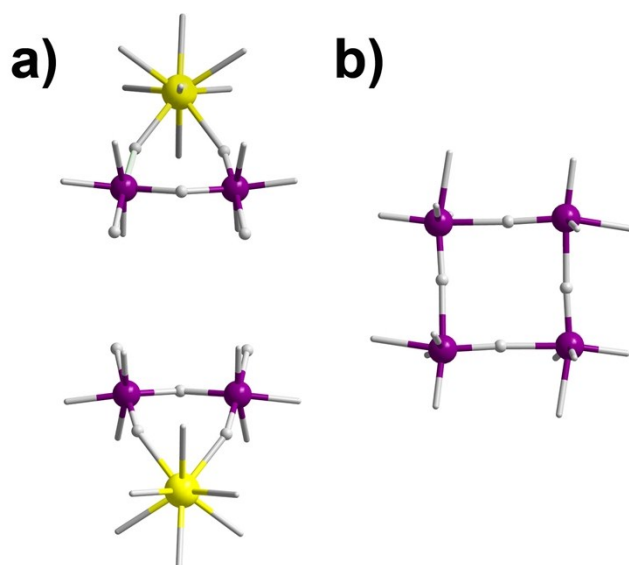**Fig. S2.** The formation structure of the $\{Ce_4Te_4W_{42}\}$ subunits.

Fig. S3. The structure of the {Ce$_4$Te$_4$W$_{42}$} subunits.

Fig. S4. The eight-coordinate Ce5 in the {Ce$_4$Te$_4$W$_{42}$} subunit.

Fig. S5. Ball-and-stick representation of the two triangle-shaped $\{CeW_2O_5(H_2O)_7\}$ linkers (right) in the center of **1a** (left).

Fig. S6. A comparative of the different linkers in Ce-containing tungstotellurites nanocluster.

2.4 The BVS Calculation Result of the Oxygen Atoms

Table S3. The BVS calculation results of the oxygen atoms in **1**.

| Oxygen Code	Bond Valence	Protonation Degree	Oxygen Code	Bond Valence	Protonation Degree
O34	0.979	1	O95	1.199	1
O68	0.319	2	O128	0.980	1
O90	1.093	1	O133	0.300	2
O92	1.105	1	O137	1.037	1
Total 20 protons per cluster					

Section 3 Experimental Section

## 3.1 Materials and Physical Measurements

Characterization: Elemental analysis of Na, Te, W, and Ce were performed with a Leaman inductively coupled plasma (ICP) spectrometer. IR spectra were recorded on an Alpha Centauri FTIR spectrophotometer on pressed KBr pellets in the range 400~4000 cm^{-1}. Water contents were determined by TG analyses on a PerkinElmer TGA7 instrument in flowing N_2 with a heating rate of 10 °C min^{-1}. X-ray photoelectron spectroscopy was performed on a VG ESCALABMKII spectrometer with an $Mg_{K\alpha}$ (1253.6 eV) achromatic X-ray source. The vacuum inside the analysis chamber was maintained at 6.2 × 10^{-6} Pa during the analysis.

Magnetic measurements: Magnetic susceptibility measurements on **1** was performed with a Quantum Design SQUID magnetometer (MPMS-XL). The dc measurements were conducted from 2.0 to 300 K at 0.1 T on polycrystalline samples. Experimental data were corrected for the sample holder and for the diamagnetic contribution of the sample, calculated from Pascal constants.

Section 4 Supplementary Physical Characterizations
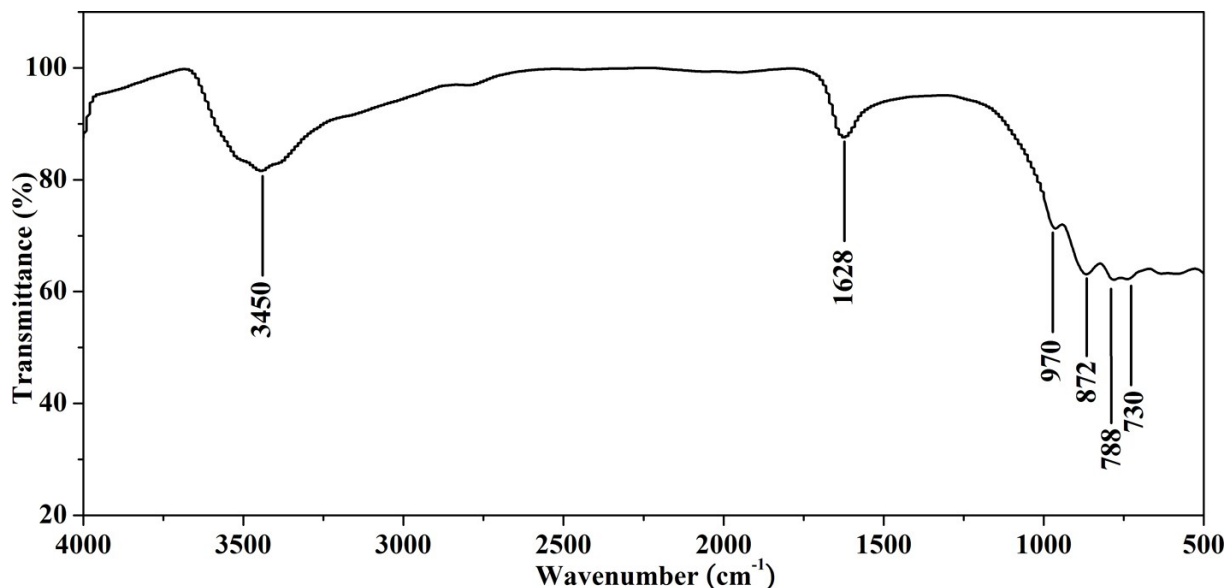
Fig. S7. IR spectrum of **1**: The characteristic peaks at 970, 872, 788, and 730 cm^{-1} are ascribed to vibrations of ν(Te–O), ν(W=Od), ν(W–Ob), and ν(W–Oc), respectively. The broad peak at 3450 cm^{-1} and the strong peak at 1628 cm^{-1} are attributed to the lattice water molecules and aqua ligands.
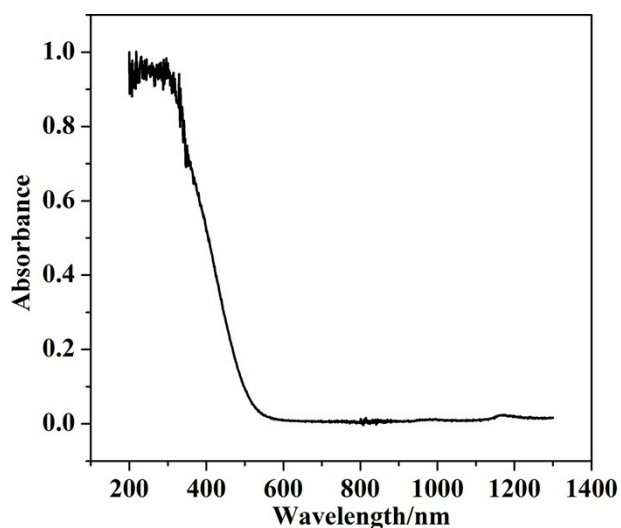
Fig. S8. UV-vis-NIR diffuse spectra of **1**. In the UV region (200 nm – 400 nm), we can find one broad peak around 300 nm, which are associated with the charge-transfer bands corresponding to $O_t \rightarrow W$ and $O_{b,c} \rightarrow W$ (*CrystEngComm*, 2014, **16**, 10746) in the polyoxoanions of **1**. In the vis (400 nm – 760 nm) and NIR (760 nm – 1100 nm) region, there was no absorption.
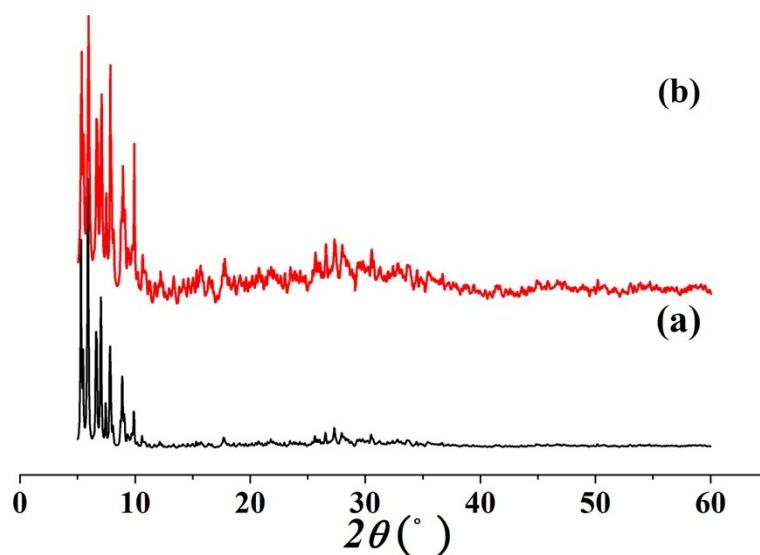
Fig. S9. The XRPD patterns for simulated (a) and as-synthesized (b) of **1**.
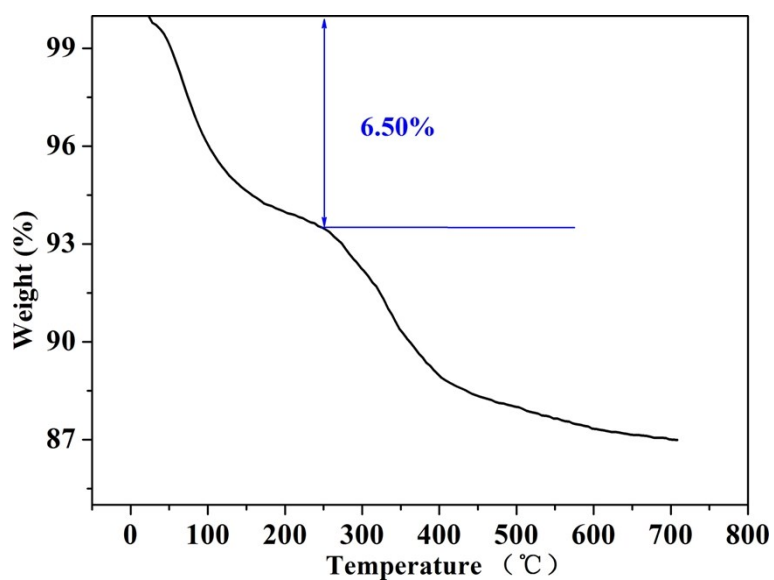
Fig. S10. TG curve of **1**. The first weight loss is in the temperature range of 50 ~ 250 °C. The value of ca. 6.50% is in accordance with the calculated value of 6.45 % (~94H$_2$O including 40 aqua ligands and 54 lattice water molecules). Then the structure begins to decompose.